EUKARYOTIC CELL, June 2003, p. 398–410 Vol. 2, No. 3
1535-9778/03/$08.00+0 DOI: 10.1128/EC.2.3.398–410.2003

Asynchronous Cell Cycle and Asymmetric Vacuolar Inheritance in True Hyphae of *Candida albicans*

Caroline J. Barelle,[1] Erin A. Bohula,[2] Stephen J. Kron,[2] Deborah Wessels,[3] David R. Soll,[3] Annette Schäfer,[1] Alistair J. P. Brown,[1] and Neil A. R. Gow[1]*

Department of Molecular and Cell Biology, Institute of Molecular Sciences, University of Aberdeen, Aberdeen AB25 2ZD, United Kingdom[1]; Department of Molecular Genetics and Cell Biology and Center for Molecular Oncology, University of Chicago, Chicago, Illinois 60637-5419[2]; and Department of Biological Sciences, University of Iowa, Iowa City, Iowa 52242[3]

Received 2 October 2002/Accepted 27 March 2003

Candida albicans **forms unconstricted hyphae in serum-containing medium that are divided into discrete compartments. Time-lapse photomicroscopy, flow cytometry, and a novel three-dimensional imaging system were used to demonstrate that the kinetics and cell cycle events accompanying hyphal development were correlated with dynamic changes in vacuole morphology and the pattern of vacuole inheritance. Apical cells of hyphae underwent continuous extension before and after the first cytokinesis event. However, the resulting mother cell and sub-apical compartments did not immediately reenter the cell cycle and instead underwent cell cycle arrest before reentering the cycle. Vacuole was inherited asymmetrically at cytokinesis so that the distal, arrested compartments inherited most vacuole and the growing apical cell inherited most cytoplasm. Hydroxyurea release experiments demonstrated that the arrested, vacuolated hyphal compartments were in the G_1 phase of the cycle. The period of cell cycle arrest was decreased by the provision of assimilatable forms of nitrogen, suggesting that the hyphal cell cycle is regulated by nitrogen limitation that results in sup-apical cell cycle arrest. This pattern of growth is distinct from that of the synchronous, symmetrical development of pseudohyphae of *C. albicans* and other yeast species. These observations suggest that the cellular vacuole space correlates with alterations in the cell cycles of different cell types and that the total organelle space may influence size-regulated functions and hence the timing of the eukaryotic cell cycle.**

Candida albicans is the major fungal pathogen of humans (5, 47) and now represents the fourth most common agent of microbial lethal septicemia in immunocompromised patients, with a morbidity of around 50% (8). Virulence of *C. albicans* is related to a combination of phenotypic traits, including its ability to form filamentous forms of either pseudohyphae or true hyphae (20). Pseudohyphae are branching chains of elongated yeast cells and are common to many dimorphic yeast species, including *Saccharomyces cerevisiae*, while true hyphae are parallel sided, are not formed by *S. cerevisiae*, and are formed only by two *Candida* species, *C. albicans* and *C. dubliniensis* (10, 13, 14, 34). The formation of true unconstricted germ tubes in serum is used in the clinical diagnosis of *C. albicans* (18, 24). Hyphal conversion has often been regarded as a virulence factor promoting tissue invasion (40, 42, 54, 58), although the true status of this morphogenetic transition as a virulence factor has yet to be evaluated fully (20, 49). Here we describe how the cell cycle of *C. albicans* is modulated during true hyphal growth. These modulations are correlated with the asymmetric inheritance of vacuole at cytokinesis, which responds to the nutrient status of the growth medium and may influence cell size-regulated functions that control cell cycle progression.

Vegetative growth of fungi occurs by the formation of either unicellular buds or branching pseudohyphae or hyphae, which ramify to form a mycelium. During growth of *S. cerevisiae* at submaximal growth rates, cell division is asymmetrical and results in buds that are smaller than the mother cell (33). The new bud has an extended G_1 period, during which the cell achieves a critical cell size that is required for the initiation of DNA replication at Start in the S phase of the cycle (34). Alternatively, many wild-type diploid strains of *S. cerevisiae* form chains of branched, elongated pseudohyphae when grown on solid, nitrogen-limited growth media (11). Pseudohyphal cells are approximately the same size at birth and undergo synchronous cell division (33). The bipolar budding pattern, typical of the diploid budding form, is a prerequisite for symmetrical, synchronous pseudohyphal development (33, 34, 74).

The cell cycle, or so-called duplication cycle, of filamentous fungi (68) occurs in the absence of cell separation but employs many of the cell cycle control elements that operate in yeast (22, 69, 74). Hyphal growth and exponential branching maximize the ability of a mycelium to assimilate nutrient-rich substrata (50, 51, 68). Some fungi display sharply contrasting programs of hyphal development in nutrient-impoverished environments that require modifications of the cell cycle. Phytopathogens, including *Uromyces* spp., *Ustilago maydis*, and *Magnaporthe grisea*, explore the relatively barren surfaces of plant host to locate appropriate sites for penetration via appressoria (27, 35). In these fungi, hyphal extension occurs in the absence of mitosis and a fixed volume of cytoplasm migrates forward with the expanding apex, leaving behind an extensively vacuolated and otherwise empty distal cell compartment (35, 64). In other fungi, such as *Basidiobolus ranarum*, cytoplasmic migration and subapical vacuolation occur while the cytoplasm in the hyphal apex expands and is divided

* Corresponding author. Mailing address: Department of Molecular and Cell Biology, Institute of Molecular Sciences, University of Aberdeen, Aberdeen AB25 2ZD, United Kingdom. Phone: 44-1224-555879. Fax: 44-1224-555844. E-mail: n.gow@abdn.ac.uk.

by cytokinesis (52). Vacuolation of sup-apical hyphal compartments in these fungi enables them to traverse or escape barren environments with minimal biosynthetic cost.

The growth and cell cycle of true hyphae of *C. albicans* differ from those of most filamentous fungi in several respects. Germ tube extension of *C. albicans* is linear, while that in true molds is exponential (15, 55, 63). In filamentous fungi, longer germ tubes have a greater capacity to generate secretory vesicles, and hence early germ tube extension rates increase in proportion to their length (68). In contrast, *C. albicans* hyphae grow with a minimal increase in the cytoplasmic volume and a substantial increase in the vacuole content of the mother cell in the first cell cycle (16, 17). Hence, linear growth of *C. albicans* hyphae reflects the constancy in cytoplasmic volume that supports germ tube extension (13). Asymmetric inheritance of cytoplasm and vacuole in subsequent cell cycles results in the elaboration of hyphae with highly vacuolated distal compartments (14, 15–17, 19, 34). Hypha formation in *C. albicans* therefore involves unequal inheritance of the vacuole at cytokinesis. In *S. cerevisiae* the inheritance of the vacuole is a spatially and temporally ordered event that is coordinated with the cell cycle. The maternal vacuole orientates itself towards the incipient bud site early in the cell cycle, forming a segregation structure that extends into the emerging bud (72). This vesicular structure persists for ~20% of the cell cycle, passing material between mother and daughter cells (12). Cell cycle-dependent polarization and subsequent directed movement of the vacuolar material are regulated by the actin cytoskeleton and are driven by the class V unconventional myosin Myo2p (26).

During the first cell cycle in *C. albicans*, nuclear division takes place in the germ tube, and then the proximal daughter nucleus migrates forward with the germ tube apex while the proximal nucleus returns to the mother cell (16, 23, 60, 65). The plane of nuclear division determines the site of the first septum (3, 15, 23, 65). In yeast and pseudohyphae, septin rings occur only at the site of mitosis that occurs at the neck of the bud and the mother cell (59, 65). During true hypha formation, a double septin ring is first seen at the site of hypha evagination prior to Start, and then later in the first cycle a second septin ring is generated at the site of mitosis within the germ tube (65). The septum always forms within the germ tube and not at the neck of the mother cell (15, 55, 65). In other respects the timings of the progression of the cell cycle events in *C. albicans* yeast cells and in the apical compartments of hyphal cells have been shown to be similar (23).

In *S. cerevisiae*, transit through the Start checkpoint requires cells to have achieved a critical cell size and access to sufficient nutrients to anticipate successful completion of a mitotic cycle (6, 45, 53). In particular, the nitrogen status of the growth medium is monitored, and an accessible source of nitrogen is required for cell cycle progression (9, 45). Size regulation at the Start cell size checkpoint of *S. cerevisiae* appears to be mediated by complexing of Cdc28 with at least one G_1 cyclin. Cln3 in particular may function as a cell size sensor (53, 70). In *C. albicans*, Cln1 is required for maintenance of hyphal development and affects the kinetics, but not the efficiency, of hypha induction (41).

In addition to exerting checkpoint control over the entry into the S and M periods of the cell cycle in *S. cerevisiae*, Cdc28p and cyclins have also been shown to control morphogenesis at these stages (7, 37–39, 44, 57). At Start the activated cyclin is involved in the subsequent induction of the evagination of the bud, while at G_2-M the active cyclin-dependent kinase is responsible for shutting down of the initial phase of polarized bud expansion and subsequent isotropic bud growth though the remainder of the cycle (37, 57). Cell cycle control and morphogenesis are therefore both regulated by the master Cdc28p kinase. The hyphal cell cycle of *C. albicans* is, however, unusual in that the polarization of actin at the time of evagination occurs before Start and hypha elongation is not regulated by events affecting cell cycle progression during budding or by Tyr19 phosphorylation of the Cdc28 cyclin-dependent kinase (23). This suggests that the morphogenetic checkpoints that are coupled to the initiation of budding in the cell cycle in *S. cerevisiae* do not operate in *C. albicans* hyphal growth.

In this study we characterized the dynamics of vacuole inheritance in relation to the growth and cell cycle of the hyphal form of *C. albicans*. We show that hyphal compartments undergo asymmetric cell cycling and that the nonbranching subapical compartments are arrested or undergo delayed transit through the G_1 phase of the cell cycle, depending on the availability of assimilatable nutrients.

MATERIALS AND METHODS

Strains and media. The clinical isolate *C. albicans* strain 3153 was used throughout (1, 15, 16). The yeast form was grown at 37°C in yeast extract-peptone-dextrose (YPD) (56). For hyphal growth, yeast cells were washed in sterile distilled water and plated onto 2% agar containing 0.1 to 20% (vol/vol) newborn calf serum (Gibco) at a density of 1×10^4 to 4×10^4 yeast cells/9-cm-diameter plate. In some experiments growth media were supplemented with glucose, amino acids, or Mycological Peptone (Difco) at the indicated concentrations. In all experiments using low serum concentrations, purified Nobel agar (Oxoid) was used to ensure minimal supplementation of the growth medium with contaminants derived from the agar.

Slide culture technique for time-lapse microscopy. Developing germ tubes and mycelia of *C. albicans* were observed at 37°C by using a slide culture technique that allowed cells to be viewed and photographed for prolonged periods without dehydration of the agar medium (32, 33). A glass slide was placed in a 9-cm-diameter petri plate, and 9.5 ml of molten serum-agar was poured into the plate to give a thin, even covering of agar over the slide. The surface of the agar was inoculated with yeast cells as described above, and a coverslip was placed over the central region of the agar to produce a thin film of inoculated agar sandwiched between the glass slide and coverslip. Agar peripheral to the coverslip was trimmed away, and the margin of the coverslip was sealed with drops of molten sealant consisting of Vaseline, lanolin, and paraffin (1:1:1). The slide was placed either in a 37°C incubator or on a heated stage of a microscope for time-lapse video microscopy. The low surface inoculation density (see above) helped prevent oxygen limitation and prevented crowding of adjacent developing mycelia. Mycelial growth was observed for up to 12 h under these conditions, and the morphology of mycelia was identical to that of mycelia generated on agar surfaces.

Time-lapse video microscopy and image analysis. Cells were examined on a Zeiss (Thornwood, N.Y.) Axioskop microscope with Nomarski differential interference contrast (DIC) optics. The microscope was placed on an antivibration table and was fitted with a video autofocus controller and stepping motor focus driver (MAC2000; Ludl Electronics Products, Hawthorne, N.J.). The temperature of the stage was controlled via warm airflow directed to the stage and a stage thermocouple. Cells were videotaped with a Hamamatsu C2400-09 Newivicon video camera (Photonics Instruments, Edison, N.J.) routed via a Hamamatsu Argus 10 video processor for background subtraction. Focused images were collected at defined intervals and recorded on an optical disk (TQ-3031F; Panasonic, Secaucus, N.J.), using a simple autofocus time-lapse image capture program (33). Cells were focused automatically immediately before each image was captured to counter thermal drift in the focal plane. In other experiments, individual video or photographic frames of mycelia were recorded at fixed intervals. Cellular parameters, compartment lengths, branching frequencies, and

numbers of compartments between the hyphal apex and the first branch were measured directly from digitized microscopic images. Cell dimensions were also calculated by using a simple video analysis system (21).

Culture methods for 3D reconstruction. For the three-dimensional (3D) reconstruction of cells and vacuoles, yeast or hyphal cells were inoculated onto a 24.5-mm-diameter coverslip coated with Cell-Tak (Sigma-Aldrich, Inc.) to facilitate adhesion. Cell-Tak was prepared in 0.1 M $NaHCO_3$ according to the specifications of the manufacturer. Loosely attached cells were gently washed off in sterile medium, and the coverslip with attached cells was assembled into a prewarmed Dvorak-Stotler chamber (Lucas-Highland, Chantilly, Va.) containing 350 μl of the desired growth medium. Yeast cells were maintained on YPD, and hyphal growth was induced with 20% (vol/vol) fetal calf serum (FCS) as described above. The chamber was then positioned on the stage of a Zeiss Axioplan upright microscope equipped with DIC optics as described below.

Optical sectioning of cells. Cells were inoculated into the Dvorak-Stotler perfusion chamber, and the chamber was positioned on the stage of a Zeiss Axioplan microscope equipped with a 100× DIC objective and a zoom tube for additional magnification. To obtain optical sections of the cells, the fine focus knob of the microscope was connected to a stepper motor programmed to take a series of optical sections in 6 to 8 s through a *z*-axis height of 5 to 10 μm (25, 61, 62, 73).

Images were recorded onto videotape through an Optronics cooled charge-coupled device camera and subsequently were entered into a Macintosh G4 computer equipped with a Data Translation (Marlboro, Mass.) frame-grabber board capable of acquiring images at 30 frames per s with Adobe Premiere software. The move was compressed into DIAS format. Optical sections of cell perimeters were outlined automatically with the pixel complexity algorithm (62). Vacuoles, nuclei, and lipid bodies were outlined by using the manual-tracing feature in the 3D-DIAS software according to the methods described elsewhere in detail (73). To generate a faceted image, the perimeters of the cell and organelles in each optical section were converted by the software to β-spline replacement images, stacked, and wrapped. Organelles were color coded and inserted into the faceted cell image to generate the composite 3D reconstruction, which could then be viewed dynamically at any angle in 3D through the Crystal Eyes 3D display system (Stereographica, San Raphael, Calif.). Control experiments demonstrated that DIC optics were able to resolve all larger vacuoles seen by FM4-64 [*N*-(3-triethylammoniumpropyl)-4-(6-(4-(diethylamino)phenyl)-hexatrienyl)pyridinium dibromide] (Molecular Probes, Eugene, Oreg.) staining of the same specimens (not shown). However, DIC optics did not resolve some of the smaller vacuoles or endosomal compartments.

Growth on endothelial cells. *C. albicans* hyphae were also observed on monolayers of bovine aortic endothelial cells (BAEs). The BAEs, generously provided by Alex Sandra, Department of Anatomy, University of Iowa, were grown according to methods described elsewhere (66), with modifications. In brief, BAEs were seeded onto sterile circular 24-mm-diameter coverslips in M199 medium at 37°C with 5% CO_2 Yeast cells of *C. albicans* 3153 were pregrown in YPD and allowed to attach to the BAEs for 15 min. Excess cells were washed off, and the coverslip was placed in a Dvorak-Stotler chamber, incubated at 37°C for 3 h, and then observed with DIC optics as described above.

HU inhibition experiments. Hydroxyurea (HU) was used to inhibit DNA replication. Mycelia were grown on slides coated with 0.01% filter-sterilized poly-L-lysine (molecular weight, 150 to 300,000; Sigma) to make them adhere to cells. The slides were submerged in liquid growth media in petri dishes and the media with or without 100 mM HU were exchanged by aspirating the medium from the dish. Cell growth was monitored with a Nikon Diaphot inverted microscope coupled to a 35-mm camera.

G_1 synchronization of yeast form cells. To obtain a homogenous unbudded population, cells were patched to YPD and grown at 25°C. After 24 to 36 h, cells were taken from the plates and inoculated at 2×10^8 cells/ml into carbon-deficient liquid medium. Optimal synchronization was obtained by using liquid synthetic complete medium lacking glucose. Following aeration at 25°C overnight, the cells were pelleted, resuspended in a small volume of water, and sonicated. Budded cells generally constituted only 3 to 6% of the resulting cultures.

Bud and hypha kinetic analyses. Once synchronized in G_1, cultures were split and exposed to either hypha-inducing or yeast form-inducing conditions. To induce germ tube formation, cells were released into liquid 1× YPD medium containing 20% fetal bovine serum (FBS) (Cell Culture Laboratories) at 2×10^7 cells/ml and 37°C. For the control treatment, synchronized cells were inoculated into YPD at 2×10^7 cells/ml and 25°C. Cells were taken from both treatments every 20 min for 4 to 6 h and fixed in 70% ethanol.

Both the YPD and FBS used in these experiments were treated with Chelex 100 (Bio-Rad), a chelating ion-exchange resin, to remove all divalent cations. This was done to reduce cellular aggregation, a characteristic of hyphal growth that limits the application of flow cytometric analysis for this growth form (28). Depletion of these cations from media significantly reduced cellular flocculation.

Flow cytometric analysis. To prepare samples for flow cytometry, ethanol-fixed cells were pelleted and resuspended in 50 mM Tris-Cl with 1 mg of RNase A per ml. Following overnight incubation with RNase A at 37°C, samples were pelleted and resuspended in 0.05 M HCl containing 5 mg of pepsin per ml for 1 h at 25°C to further reduce cellular aggregation. Following protease treatment, cells were stained in a solution containing 180 mM NaCl, 70 mM $MgCl_2$, 180 mM Tris-Cl, and 0.05 mg of propidium iodide per ml at room temperature for 1 h. Flow cytometer preparations were stored at 4°C for up to 48 h. Just prior to analysis, the samples were sonicated to separate cells. Data were collected by using a FACSCalibur cytometer (Becton-Dickinson, San Jose, Calif.) and analyzed with Cell Quest 3.0 software.

Aliquots from the samples prepared for flow cytometry were used to determine germ tube growth rates in 20% FBS–YPD medium at 37°C. Photographs were taken with an Axiovert 25 inverted phase microscope (Zeiss) and a Pixera (San Francisco, Calif.) Professional camera with a 40× objective. At least 60 independent cells were measured for each time point. The resulting data were compiled and analyzed by using StatView 4.5.

Vacuole and nuclear staining. Vacuoles were stained with the vital stain FM4-64 as described previously (26, 71). Yeast cells or hyphal-phase cells were suspended in YPD or 20% (vol/vol) serum, respectively, containing 80 μM FM4-64 for at least 60 min before being examined under fluorescence and excited at 488 nm. To visualize nuclear events during germ tube growth, cells were synchronized and data were collected at various time points as described above. Cells were fixed in 3.7% formaldehyde at room temperature for a minimum of 3 h. Samples were then washed three times with a buffer containing phosphate-buffered saline and 1% Triton X-100 and stained for 1 h at room temperature in 0.8 mg of DAPI per ml (4′,6′-diamidino-2-phenylindole) in phosphate-buffered saline and 1% Triton X-100. After being stained, cells were washed three times with the buffer and Nomarski and DAPI pictures were taken with an Axioskop microscope (Zeiss), a SenSys camera (Photometrics, Tucson, Ariz.), and IP Lab Spectrum 3.1 software (Signal Analytics, Vienna, Va.).

RESULTS

Yeast form cell cycle kinetics. In order to evaluate modifications in the cell cycle in yeast and hyphal forms of *C. albicans*, several parameters were first assessed in the budding yeast form. To study yeast form kinetics, stationary-phase cells in which only 3 to 6% of cells were budded were used as an inoculum for growth under non-hypha-inducing conditions in liquid YPD at 25°C. These cells were shown by flow cytometry to be in G_1. Budding indices were analyzed for 6 h following release. The growth rate over the first cycle under these conditions was lower than that for mid-exponential-phase yeast cells growing in YPD at 25°C. Inoculation into YPD did not result in a quick or uniform reentry into the cell cycle. Instead, the proportion of small budded cells increased slowly over 200 min before peaking at only 30% (Fig. 1). Flow cytometry of these cells showed that a small number of cells began DNA replication after 80 to 100 min. For the next 4.5 h, the number of cells in S phase changed little. Over time, the majority of cells accumulated in G_2; however, the G_1 peak was never completely lost (Fig. 2A). At later time points, 37% of the cells were large and budded, 20% were small and budded, and 43% were unbudded, suggesting that the culture was cycling asynchronously.

Growth of synchronized germ tubes in the first hyphal cycle. G_1 synchronized yeast form cells were induced to form germ tubes by release into liquid 20% (vol/vol) FCS medium at 37°C. Hyphal cells were fixed, photographed, and prepared for flow cytometry at intervals following exposure to serum (Fig. 1 and 2). Samples collected before 30 min showed little growth. After a short lag in the growth rate, the mean germ tube length

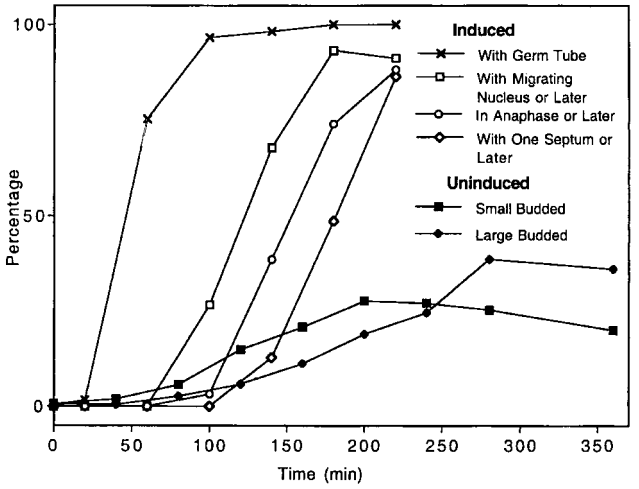

FIG. 1. Yeast and hyphal growth forms display different cell cycle kinetics. Indices describe bud morphology after release of yeast cells synchronized in G_1 from in minimal medium lacking a carbon source into YPD at 25°C and show slow asynchronous reentry into the cell cycle, with data for small and large buds scored separately. Germ tube emergence in G_1-synchronized yeast form cells released into YPD with 20% serum at 37°C displays an initial lag followed by a nearly synchronous increase. Indices of nuclear migration, anaphase, and septation in the first cell cycle are also shown.

increased linearly over the course of the first cell cycle (data not shown) (15, 17). Regression analysis of the data for the later time points after germ tube formation was complete produced an average linear extension rate of 0.35 μm/min (r^2, 0.994), which is closely comparable with published values (15, 17, 55).

The cell cycle kinetics of both synchronized budding and hyphal cells were analyzed by using flow cytometry and nuclear staining. Yeast cells arrested in G_1 were released into liquid YPD with 20% FCS at 37°C or into yeast form-inducing YPD at 25°C. Chromosomal staining revealed a clear progression of nuclear events over the first yeast and hyphal cycle. Mitosis took place at the neck of the mother and bud of yeast cells (Fig. 3A). During hyphal growth, the nucleus migrated from the mother cell into the germ tube. Migration stopped once the nucleus traveled one-third to on-half of the length of the germ tube (Fig. 3B). The nucleus then elongated as the cell entered anaphase. The postmitotic nuclei segregated, and the proximal nucleus migrated back to the base of the germ tube (Fig. 3B). Upon reaching the mother cell, the migrating nucleus lost its elongated shape (Fig. 4). Septa were visible before the subapical nucleus reached the mother yeast cell (Fig. 4A). In further cycles, the postmitotic distal daughter nucleus remained near the septum and the distal nucleus migrated forward with the apex (Fig. 4B and C).

A combination of flow cytometry analysis and microscopy data enabled the approximate timing and sequence of events in the first hyphal cycle to be described. Hypha-induced cells started DNA replication 60 to 70 min after inoculation (Fig. 2B), when greater than 70% of the cells had formed germ tube evaginations (Fig. 1). The S phase occurred between 100 and 140 min, after which time nuclear migration occurred. By 150 min, more than 50% of the cells were either in or past anaphase (Fig. 1 and 2B). Thirty minutes later, more than 50% of the cells had formed septa. At the later time points, flow cytometry data suggested that some of the cells had reentered the cycle and were replicating their DNA.

Time-lapse analysis of germ tube formation. Early reports had shown that mother cells supporting germ tubes had large vacuoles (16, 34). The relationship between germ tube growth and vacuole inheritance was studied by time-lapse video microscopy with asynchronous yeast cells as an inoculum and

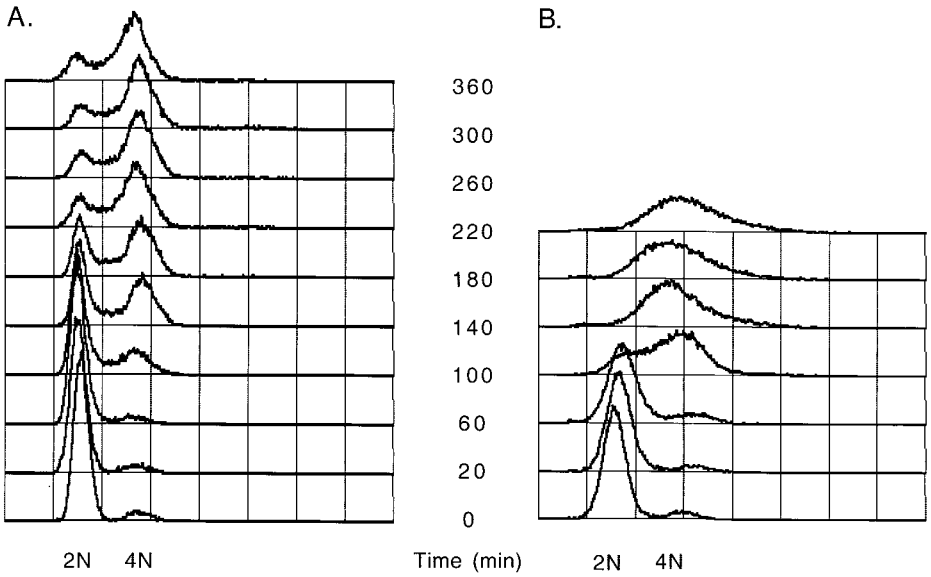

FIG. 2. Flow cytometry analysis of kinetics of the first hyphal cycle. Wild-type yeast form *C. albicans* cells were synchronized in G_1 by carbon starvation in minimal medium and then released into YPD or YPD with serum at 37°C. (A) Profile after release into YPD, showing asynchronous onset of DNA replication and return to a cycling yeast form cell cycle. (B) Profile after release into serum reveals a faster and more uniform onset of DNA replication.

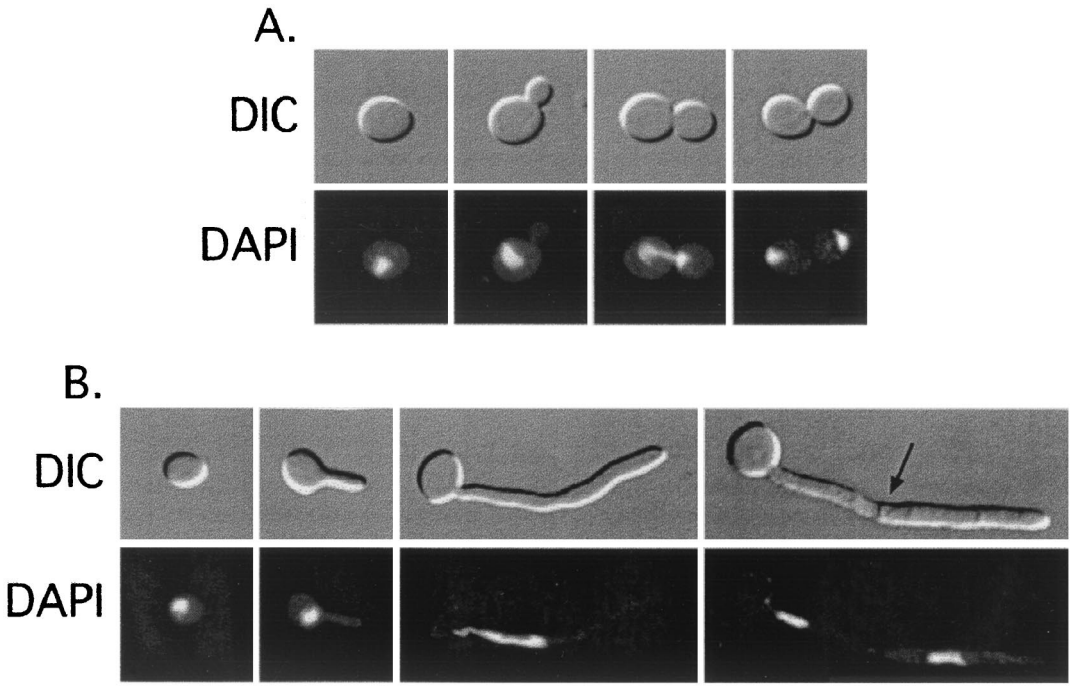

FIG. 3. DIC and DAPI-stained fluorescence micrographs of *C. albicans* cells at various stages of the yeast form (A) and first hyphal (B) cell cycles. Cells were synchronized in G_1 via carbon starvation and released into noninducing (1× YPD at 25°C) or inducing (1× YPD containing 20% FBS at 37°C) conditions. From left to right: G_1 phase, S phase, anaphase, and telophase cells (A) and G_1 phase, S phase, anaphase, and septate cells (B). The arrow points to a septum. Magnification, ×760.

agar containing 20% (vol/vol) FCS. As in liquid cultures, germ tubes developing in agar arose from mother yeast cells within 30 min and over 90% of cells formed germ tubes within an hour. The development of an extensive vacuole in the parental yeast cell was observed (Fig. 5, 1 to 100 min), and dynamic changes in vacuole morphology were seen as the germ tube emerged. By the end of the first cell cycle when the first septum was laid down, the parental cell typically had a large central vacuole, whereas the germ tube had little or no vacuole that could be imaged by DIC optics. Septation represents complete cell cytokinesis, since the septum of *C. albicans* has only a narrow central micropore that is too small to permit passage of organelles or cytoplasm between adjacent compartments, (18). During the second cell cycle, extension of the apical cell continued at a linear rate, but on 1% (vol/vol) serum agar a second germ tube was not formed until after the second septum had been produced (Fig. 5, 100 to 180 min). The hyphal compartment formed after the second septum was laid down did not branch until the apical cell had undergone a further cell cycle (Fig. 5, 240 min). Therefore, under these conditions, septation

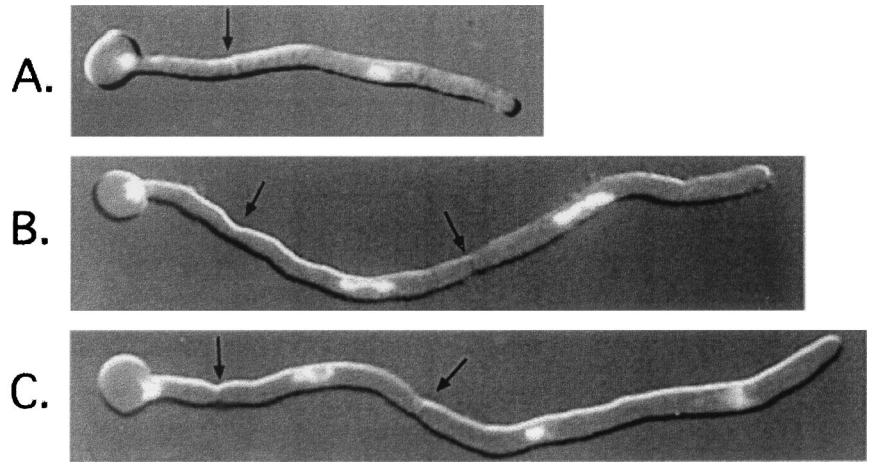

FIG. 4. Nuclear division in the apical cell of *C. albicans* hyphae. (A) Completion of first cycle; (B) second cycle; (C) telophase of third cycle. Subapical cells display a protracted G_1 arrest with no evagination of the mother cell in panel C, even after the near completion of three cycles in the germ tube. Arrows point to septa. Magnification, ×1,010.

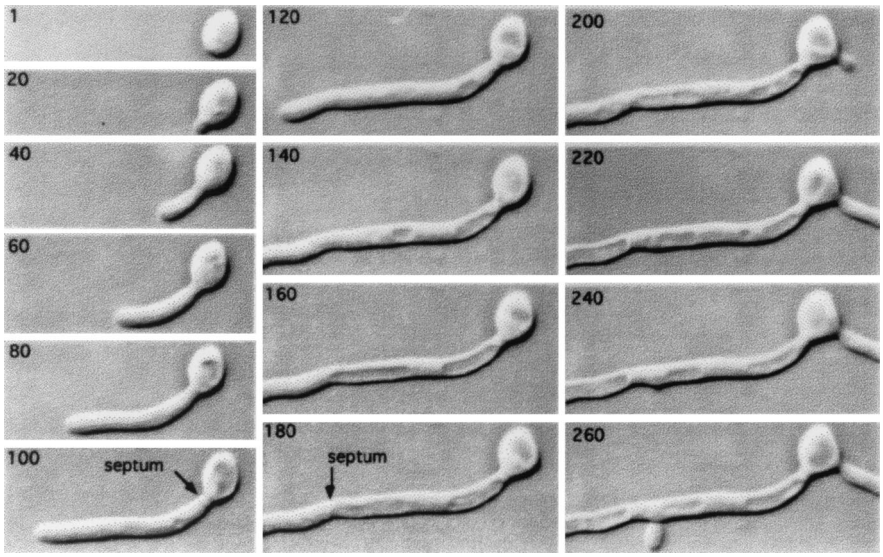

FIG. 5. Time-lapse video recordings of a germ tube of *C. albicans* growing on 1% (vol/vol) serum agar at 37°C. The elapsed time in minutes is shown in the top left of each micrograph, and the formation of the first and second septa is indicated. In panels from 80 to 100 min the enlarging vacuole is seen clearly within the parental yeast cell. Vacuoles are also evident behind the expanding germ tube apex so that the formation of the second septum within the germ tube creates an intercalary compartment that is extensively vacuolated with a central cytoplasmic region containing the nucleus. The parental yeast cell formed a second evagination at 190 min, corresponding to the third division cycle of the primary germ tube. The vacuole in the proximal region of the subapical compartment was no longer evident by the time the first branch was formed at 235 min. Magnification, ×880.

was followed by cell cycle arrest in all subapical compartments, including the parental yeast cell. Cell division of the hyphal apical cell relative to the subapical daughter yeast cell or daughter hyphal compartment is therefore asynchronous.

During germ tube extension of the apical cell, the proximal hyphal compartment became increasingly vacuolated, but apical regions contained few vacuoles (Fig. 6c and d). The second septation event resulted in most of the vacuole being inherited by the subapical intercalary compartment (Fig. 5 and 6a and b). These compartments normally had a nonvacuolated central region representing the position of the central nucleus (Fig. 6a and b). Vacuoles were not seen in the apices of emerging of branches or secondary germ tubes, and a decrease in the proportion of vacuole to total cell volume was evident in growing compartments (Fig. 5). Therefore, large vacuoles were inherited predominantly by parental cells after cytokinesis, and nongrowing compartments were extensively vacuolated (Fig. 7). This pattern of vacuolation was also observed in hyphae that developed in endothelial tissue cultures (Fig. 8), suggesting that these observations are also relevant to growth of *C. albicans* in vivo.

Vacuole dynamics. In order to image the spatial and temporal pattern of vacuolation during germ tube development, we used the 3D-DIAS program, which uses edge detection of DIC images from serial sections to continuously reconstruct the cell architecture (25, 61, 72). Control experiments with the vacuole stains FM4-64 and CDC-FDA confirmed that the DIC images properly identified vacuole compartments (not shown). Lipid bodies were also prominent in DIC sections (Fig. 9). During the first cycle, the 3D-DIAS faceted reconstructions again showed an expanding vacuole compartment within the parent mother cell (Fig. 9). The major vacuole was resolved in 3D as a spheroid or lobed structure with a constricted waist. The overall vacuole shape was dynamic and changing even in subapical compartments that had no secondary germ tube or branch (Fig. 9 and 10). Vacuoles not only expanded but also underwent regular simultaneous fusion and fission events (Fig. 10). Smaller vacuoles were observed to migrate in both anterograde and retrograde directions, while the larger, developing distal vacuole remained in a relatively constant periseptal location (Fig. 10).

Branch formation regulated by serum concentration. The delay between cytokinesis and the formation of a germ tube or branch in the newly formed subapical compartment was dependent on the serum concentration (Fig. 11A and C). For example, at a serum concentration of 1% (vol/vol), the branching frequency was almost half of that in 20% serum as determined by the number of compartments between the apical cell and the first hyphal compartment with a lateral branch. Since this growth medium contained only serum and agar, we conclude that the lack of accessible (low-molecular-weight) nitrogen and carbon suppressed branch formation and extended the delay in the cell cycle in hyphal compartments. The length of hyphal compartments was related inversely to serum concentration, with compartments of hyphae grown in 20% (vol/vol) serum being 20% shorter than those formed in 1% serum (not shown). After an extended period of growth on serum agar, mycelial colonies reverted to growth by budding at septal junctions. Reversion to budding was most rapid on media with low serum concentrations (not shown).

Induction of branching by nitrogen sources. We reasoned that the cell cycle delay we observed in hyphal compartments of hyphae growing in serum-containing agar may be due to inadequate provision of assimilatable low-molecular-weight nutrients. Therefore, low-serum agar was supplemented with various nitrogen and carbon sources and the effect on branch-

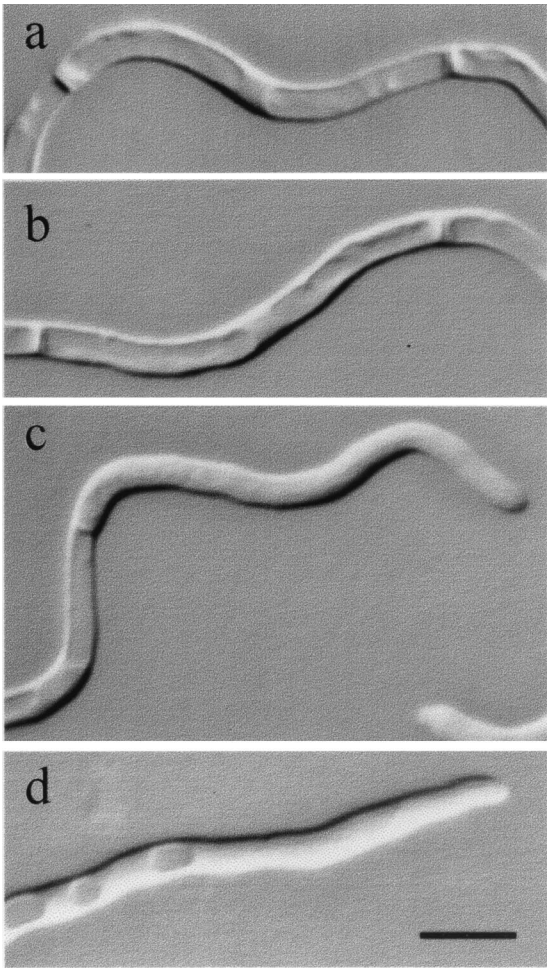

FIG. 6. Vacuole formation in hyphal compartments of mycelia grown on 1% (vol/vol) FCS, showing highly vacuolated intercalary compartments (a and b) and nonvacuolated hyphal apices (c and d). Bar, 5 μm.

ing frequency was assessed. Addition of mycological peptone reduced the number of compartments to the first branch (Fig. 11B) and increased the branching frequency but did not affect the compartment length (not shown). Branches were also formed at a more apical position relative to the proximal end of compartments in the presence of peptone. Similarly, amino acids also reduced the number of compartments before the first branch (Table 1). Mixtures of two or three amino acids tested at 100 μM each were added to 0.5% serum agar. All amino acid mixtures caused a significant reduction in the mean number of compartments before the first hyphal branch, although the aliphatic and aromatic amino acid mixtures were less effective than other amino acid groups (Table 1). In addition, treatment of 0.5% (vol/vol) newborn calf serum, used to induce hyphal formation, with trypsin reduced the number of compartments to the first branch or bud by almost 50% (Table 1). Treatment of the newborn calf serum with heat-inactivated trypsin did not affect branching. These experiments suggest that the provision of assimilatable nitrogen in the form of peptone, amino acids, or proteinase-digested serum all decreased the cell cycle delay in hyphal compartments as determined by measurement of the timing of branching.

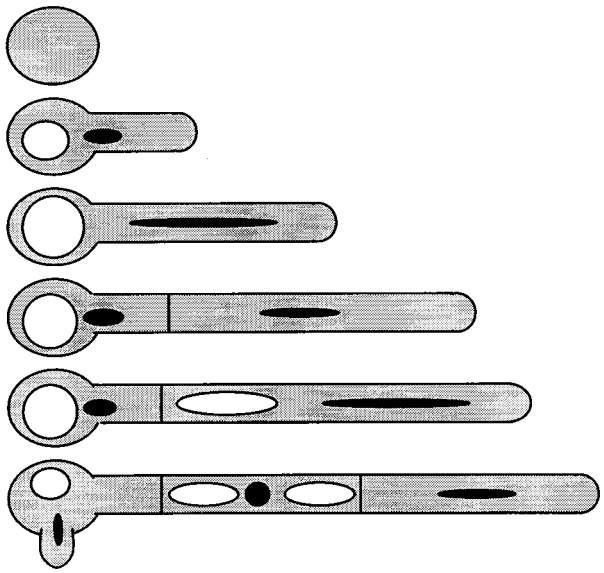

FIG. 7. Asymmetric cell division of *C. albicans*, leading to an asynchronous cell cycle and sustained apical growth but delayed branching. During the first hyphal cycle an increase in vacuolation is seen in the mother cell. Upon septation, the subapical cell inherits the majority of the vacuole, while the tip cell receives most of the cytoplasm. At this point, the tip cell reenters the cell cycle as the subapical cell undergoes protracted G_1 arrest. This phenomenon is repeated in each subsequent division at the tip. Sup-apical cells bud or branch only after the vacuole has shrunk significantly. An increase in cytoplasmic volume in hyphal compartments precedes branching.

In contrast, addition of up to 1% glucose to 0.5% serum agar had no effect on the number of hyphal compartments before the first branch (Fig. 11B). There was a small but significant decrease in the mean number of compartments before the first branch with a supplement of 4% glucose to this medium (Fig. 11B). Addition of glucose did not affect the polarized positioning of branches towards the proximal end of each compartment or the compartment length (not shown). Therefore, cell cycle arrest in subapical hyphal compartments is more strongly influenced by nitrogen availability than by carbon availability.

Subapical compartments are arrested in G_1. Since subapical compartments and parental yeast cells did not reenter the cell cycle after septation and cytokinesis, we tried to establish the phase of the cell cycle at which nongrowing hyphal compartments were arrested. *C. albicans* yeast cells that are induced to form hyphae adhere to one another avidly, forming multicellular aggregates. Despite numerous attempts, this autoaggregation phenomenon prevented use of flow cytometry to establish the pattern for the increase in nuclear content over the first two hyphal cycles. We reasoned that the nuclear content would increase from 2n to 3n (for G_1-arrested mother cells) or from 2n to 4n (for G_2-arrested cells). Quantitative fluorescence imaging of DAPI-stained nuclei was found not to be sufficiently sensitive to distinguish the DNA contents of apical and subapical nuclei in hyphal compartments. DAPI-stained hyphae showed that in no case had the nucleus undergone mitosis prior to the time of branch formation (not shown).

Mycelia were grown on poly-L-lysine-coated glass slides in petri dishes containing 0.5 and 1% (vol/vol) serum for 16 h. These mycelia had few branches (Fig. 12a). The low-serum

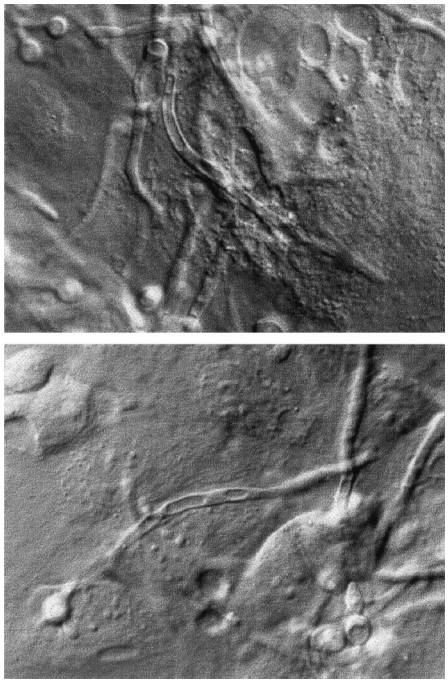

FIG. 8. Vacuole formation in hyphae grown on a confluent cell culture of BAEs. Magnification, ×550.

medium was then removed and replaced with 20% (vol/vol) calf serum with and without 100 mM HU. Mycelia in the absence of HU were stimulated to form branches (not shown). In the presence of HU, the apical compartment continued to grow for a period until the S phase of the next cycle and then stopped. Subapical branching was prevented in the presence of HU despite the presence of 20% serum (Fig. 12b). Upon removal of the HU, the apex eventually resumed growth and each of the subapical compartments formed branches or lateral buds (Fig. 12c). Since HU inhibits DNA synthesis during the S phase, this suggested that subapical compartments formed in low-serum medium had not gone through the S phase of the cell cycle and were therefore most likely to be arrested in the G_1 phase of growth. Control cultures in which 20% serum was added without HU formed branches within 2 h (not shown).

DISCUSSION

True hyphae and pseudohyphae of *C. albicans* are distinct growth forms. Our analysis demonstrates that the cell cycle characteristics of true unconstricted hyphae of *C. albicans* are distinct from those of the yeast and pseudohyphal forms of *C. albicans* and *S. cerevisiae* (74). The bipolar budding of diploid *S. cerevisiae* strains is asymmetrical and asynchronous at all submaximal growth rates, while pseudohyphal growth is characterized by symmetrical and synchronous division of constituent cells (33, 34, 74). The vacuole volumes in pseudohyphae of mother and daughter cells of *C. albicans* at cytokinesis appear to be similar (75). It has also been reported that sizes of yeast cells at pseudohyphae at cell division were similar if vacuolar volume was omitted (75). In *C. albicans*, hyphal cell division is defined by regular septation, which is asymmetric since cytoplasm is partitioned predominantly to the proximal apical cell and most vacuole is inherited by the subapical mother yeast cell or hyphal intercalary compartment. Cell division is also asynchronous, since subapical compartments arrest in the cycle for a period that may extend for times equivalent to five to six cell cycles under the conditions described in this study. This asynchrony in the hyphal cell cycle adds to a list of features that distinguish true hyphae and pseudohyphae (reviewed in reference 14).

Recent work with *S. cerevisiae* has shown that the shaping of buds is regulated by morphological checkpoints triggered by the phosphorylation of Tyr19 and the association of Cdc28/2 cyclin-dependent kinase with appropriate G_1 or G_2 cyclins at Start and at the G_2/M transition prior to mitosis (37–39, 57). Swe1-dependent phosphorylation of Cdc28 Tyr19 is proposed to delay the transitions from polarized to isotropic growth of *C. albicans* (23, 41), resulting in the extension of pseudohyphal development (7). Therefore, elongation and the shape of yeast cells during bud and presumably pseudohyphal growth are regulated by the cell cycle. However, it was shown recently that the elongation of true hyphae of *C. albicans* was not regulated by Try19 phosphorylation of Cdc28, suggesting that hypha morphogenesis and the cell cycle are regulated in parallel in this growth form (23). Our results suggest that hyphal growth also involves additional controls over vacuole inheritance and the regulation of cytokinesis.

Vacuole compartment size influences size-regulated cell cycle functions. Cell size influences the progression of the cell cycle (53). Recently it was shown that deletion of around 500 genes in *S. cerevisiae* affected cell size distributions (31). *C. albicans* yeast cells in phases other than G_1 could be induced to form hyphae (23). We have shown that highly vacuolated cell compartments are likely to be arrested in G_1, since branch formation could not be induced in such compartments by the addition of nutrients in the presence of HU. It is formally possible, however, that additional cell size-regulated control is also exerted at G_2, which again could be influenced by vacuole volume. These observations are resolvable by hypothesizing that yeast cells and pseudohyphae normally have sufficient cytoplasm to support cell evagination, while arrested hyphal compartments are extensively vacuolated and have insufficient cytoplasm to execute cell size-mediated events leading to cell evagination. We observed that the vacuole volume of such compartments is reduced prior to reentry into the cell cycle. We suggest, on the basis of our observed correlation between vacuolation and cell cycle progression, that arrested cells are too vacuolated or have too small a cytoplasmic volume to execute the size-dependent S function at the G_1/S transition and that this is required for hyphal compartments to reenter the cell cycle. This leads to a refinement of the concept of size-regulated cell cycle control such that the cell size is related to its cytoplasmic volume minus the vacuole (and other organelle) space rather than total cell volume. For most cells, symmetric cell division results in an approximately equal segregation of organelle compartments between daughter cells. Therefore, the ratio of total cell volume to nonorganelle cell volume would be a constant. However, the asymmetric cell division associated with germ tube growth in *C. albicans* results in cells so extensively vacuolated that they evidently have to regenerate cytoplasm de novo at the expense of vacuole before they are able reenter the cell cycle. In *Schizosaccharomyces*

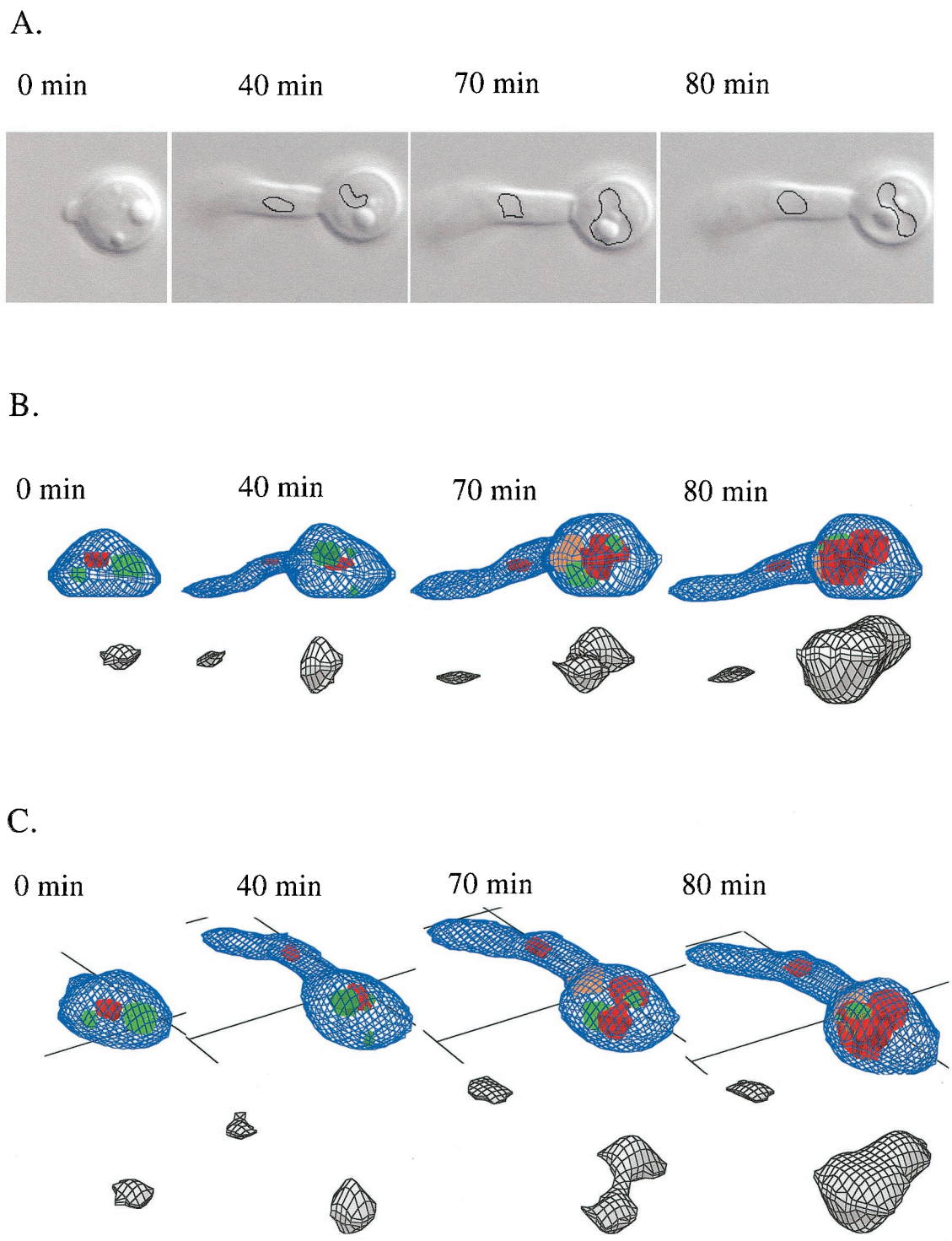

FIG. 9. Reconstruction of the cytology of germ tube formation and vacuole formation by using a 3D-DIAS imaging system. DIC images (A) were used in an edge detection program to outline the vacuole in serial DIC sections (black lines) and then construct faceted images (B and C). The vacuole is shown in green, or in gray when shown separately. Lipid bodies are in red, and the first septum is in orange. The same germ tube is shown as observed from the side at 0° (B) or at 30° (C).

pombe, cell size regulation is exerted at G_2/M rather than the G_1/S interface as in *S. cerevisiae* (46) and in *C. albicans*, as shown here. Consequently, stationary-phase cells of *C. albicans* and *S. cerevisiae* accumulate at G_1, prior to Start, while *S. pombe* cells accumulate at G_2. In other yeasts, such as *Cryptococcus neoformans*, stationary-phase cells have a bimodal size distribution representing cells that are arrested in either G_1 or G_2 (67).

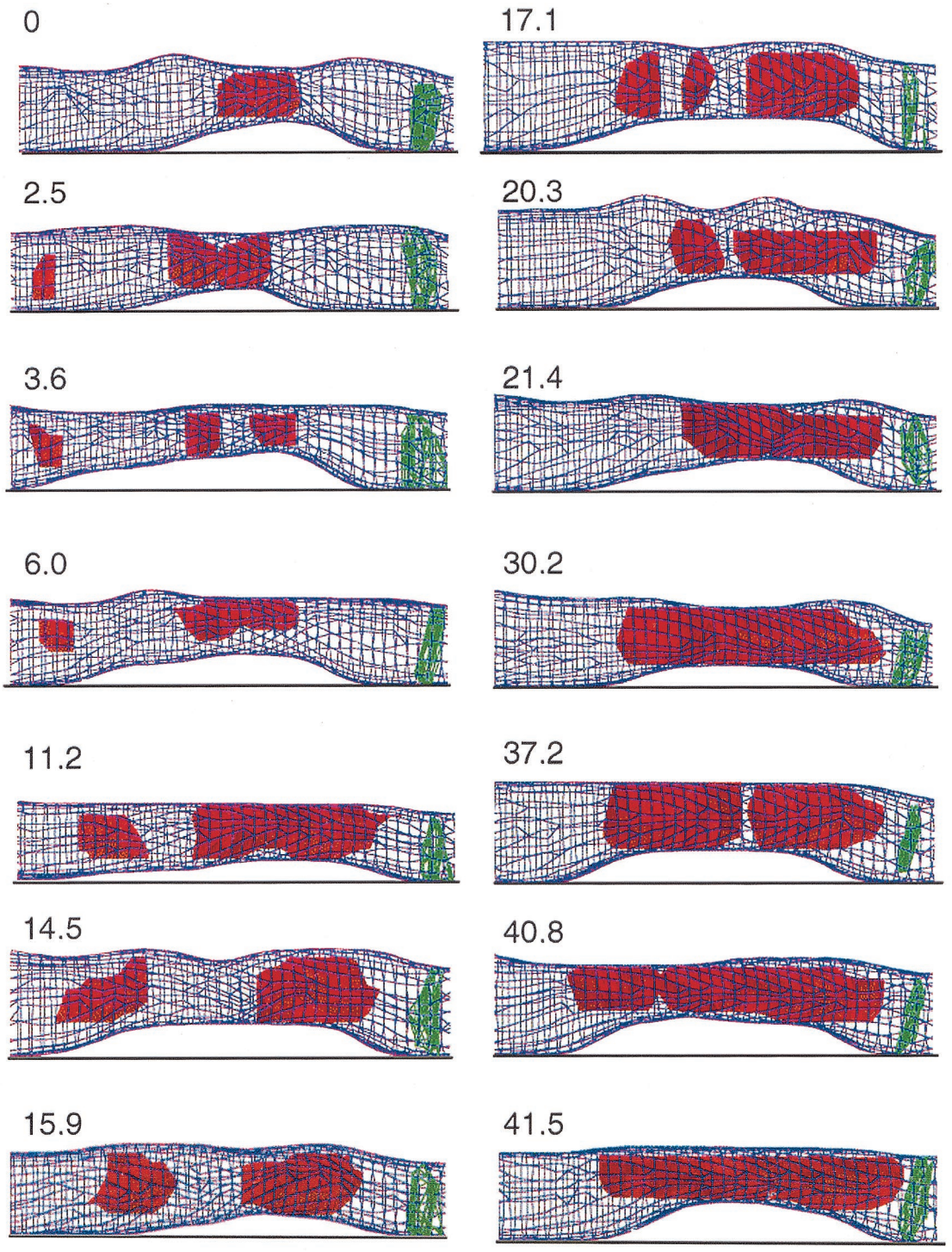

FIG. 10. Vacuole dynamics in distal region of apical hyphal cell. The elapsed time is indicated in minutes for each faceted reconstruction. The vacuole is in red, and the septum is in green. The apex is to the left side of the image. Rapid migration, fusion, fission, and enlargement of vacuoles are seen to create a large periseptal vacuole that will be inherited predominantly by the subapical daughter cell following cytokinesis.

Hypha formation as a response to nitrogen starvation. Cell cycle reentry in arrested hyphal compartments was found to be accelerated by provision of amino acids or peptone or by peptides generated by the partial hydrolysis of newborn calf serum used to induce hyphal growth. These observations are consistent with such compartments being arrested in G_1 due to nutrient limitation (45). Many reports have suggested that growth media that stimulate hyphal growth are poor in nitrogen (4, 13, 47, 49) and that hyphal growth imparts the property of motility to a sessile cell, therefore allowing it to escape nutrient-impov-

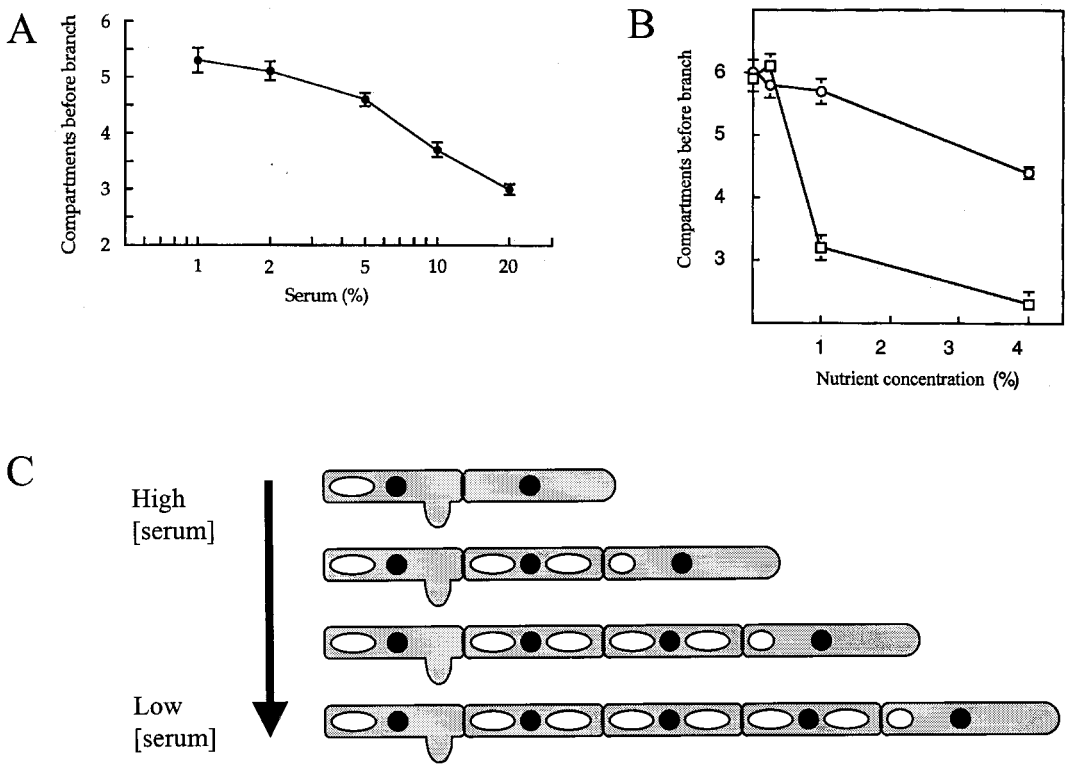

FIG. 11. (A) Relationship between newborn calf serum concentration and delay before hyphal branching as determined by measurement of the average number of hyphal compartments before the first branch. Error bars indicate standard errors of the means ($n = 20$). (B) Effect of addition of peptone (□) and glucose (○) to 0.5% newborn calf serum agar on the delay of branching of *C. albicans*, as measured as the mean number of hyphal compartments to the first branch. Error bars indicate standard errors of the means ($n = 7$). (C) Schematic representation of the effect of medium serum concentration on the branching of mycelia of *C. albicans*. Low serum concentrations cause cell cycle arrest and delayed cell cycle reentry.

erished environments (11, 13). Since the morphology of hyphae found in biopsies of clinical material is often sparsely branched (5, 20, 48), this suggests that the in vivo growth environment is relatively nutrient poor. Although sera are rich in soluble protein and induce hyphal development, the nutrients in sera are present mainly a nonaccessible form. Proteins are hydrolyzed by aspartyl proteases (29) to generate short oligopeptides that can be taken up by *C. albicans* peptide permeases (2, 30, 43). This is consistent with the observations reported here that enrichment of serum with amino acids, peptone, and peptide hydrolysates all accelerated reversion to vegetative growth by budding. The ability of moderate concentrations of serum incorporated into solid media to sustain hyphal development for longer periods than other laboratory media is therefore likely to be due to the fact that the ramifying hyphae are always entering fresh, nonhydrolyzed serum at the colony margin. Hyphae revert more quickly to yeast forms in liquid media and when any assimilatable form of nitrogen is provided with the serum. Media such as that described by Lee et al. (36) are rich in amino acids and combined nitrogen and rely on changes in external pH and temperature to stimulate the dimorphic transition. Reversion to yeast-like growth in these media is rapid, and true hyphal branches are rare after only a few hours of filamentous growth (19).

Therefore, as in *S. cerevisiae*, hyphal growth of *C. albicans* is a foraging response to low-nitrogen environments. We propose that the formation of vacuolated, G_1-arrested, subapical compartments during hyphal growth minimizes the requirement for protein synthesis under such nitrogen-poor conditions. When secreted proteases enrich the medium with assimilatable peptides, de novo protein synthesis re-

TABLE 1. Effect of different nitrogen sources on branching frequency in *C. albicans* hyphae

Treatment	Supplements	No. of hyphal compartments before first branch[a]
Control (0.5% [vol/vol] serum)		5.9 ± 0.2
Amino acids	Val-Leu-Ile	5.1 ± 0.2
	Gly-Ala-Pro	3.4 ± 0.1
	Ser-Met-Thr	4.0 ± 0.2
	Cys-Asn-Gln	3.5 ± 0.1
	Phe-Tyr-Trp	5.3 ± 0.3
	His-Arg-His	3.7 ± 0.1
	Asp-Glu	3.8 ± 0.1
Trypsin[b]		3.4 ± 0.2
Heat-inactivated trypsin		5.4 ± 0.5

[a] Mean number of compartments from the hyphal apex to the first branch in 0.5% (vol/vol) serum agar with mixtures of various nitrogen supplements. Values are means ± standard errors ($n = 14$) from two independent experiments. The standard error for the control is from seven independent experiments ($n = 49$), and the trypsin results are based on a single experiment ($n = 15$).

[b] Newborn calf serum (0.5%) was digested with 10 μg of trypsin per ml for 16 h at 37°C and then heat-inactivated (76).

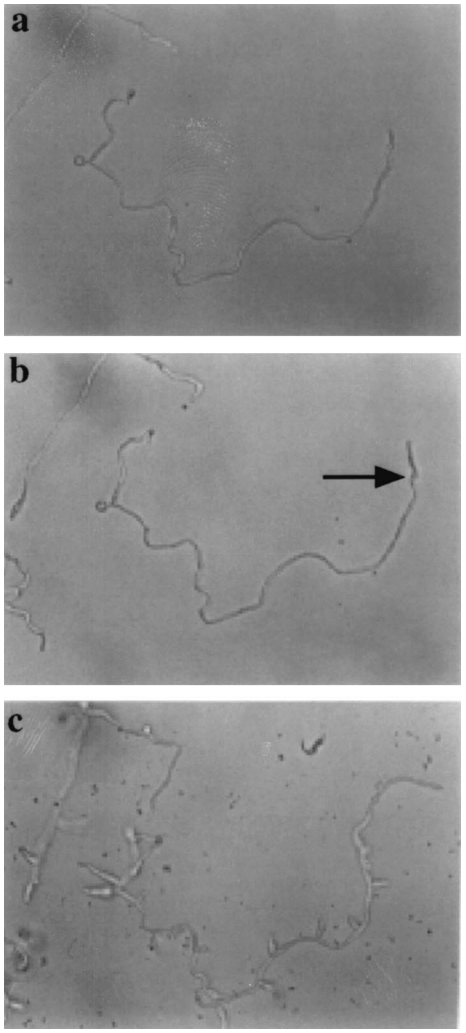

FIG. 12. HU release experiment demonstrating G_1 arrest of hyphal compartments, as described in the text. (a) Morphology of a sparsely branched mycelium after 16 h of growth in 0.5% serum. (b) The liquid serum medium was removed, and the mycelium was photographed 15 h after transfer to 20% serum medium with 100 mM HU. The apical cell (arrow) grew for one cell cycle and then arrested. The apex of the hypha on the left of the micrograph is out of focus above the plane of the dish. (c) Stimulation of branch-lateral bud formation is shown 10 h after removal of the HU in the continued presence of 20% serum. Since compartments could not form branches in the presence of HU, they are arrested in the G_1 phase of growth, prior to S. Magnification, ×200.

generates sufficient cell cytoplasm for the cell to exceed the size-mediated requirement for the execution of Start. Intercalary hyphal cells then reenter the cell cycle and form evaginations that may form lateral branches or, under more highly nutrient-enriched conditions, lateral buds. The spatial dynamics of vacuole formation and inheritance therefore correlate with cell cycle timing and thus may play a critical role in the cell cycle and hyphal development of *C. albicans*. Therefore, we are now undertaking an analysis of the genetic regulation of vacuole inheritance in relation to hyphal development in this organism.

ACKNOWLEDGMENTS

We acknowledge Gerald Fink and Lois Weisman for their critical contributions to this work and their help and advice. We thank Edward Voss, Carla Daniels, and Amanda Wood at the W.N. Keck Dynamic Image Analysis Facility at the University of Iowa.

Initial studies were supported by NIH grant GM40266 to G. R. Fink. The W.N. Keck Dynamic Image Analysis Facility at the University of Iowa is supported in part by NIH grant HD1A577. S.J.K. and E.A.B. were supported by a Beckman Foundation Young Investigator Award and NSF career award MCB-9875976. Personal fellowships to N.A.R.G. from the Royal Society of Edinburgh/Caledonian Research Foundation and Royal Society/Leverhulme Trust are acknowledged gratefully, as is financial support from the Wellcome Trust (grants 039643 and 063204) and BBSRC (grants 1/CEL 04556 and 1/0014870).

REFERENCES

1. **Anderson, J., and D. R. Soll.** 1986. Differences in actin localization during bud and hypha formation in the yeast *Candida albicans*. J. Gen. Microbiol. **132:**2035–2047.
2. **Basrai, M. A., M. A. Lubkowitz, J. R. Perry, D. Miller, E. Krainer, F. Naider, and J. M. Becker.** 1995. Cloning of a *Candida albicans* peptide transport gene. Microbiology **141:**1147–1156.
3. **Bedell, G. W., A. Werth, and D. R. Soll.** 1980. The regulation of nuclear migration and division during synchronous bud formation in released stationary phase cultures of the yeast Candida albicans. Exp. Cell Res. **127:** 103–113.
4. **Brown, A. J. P., and N. A. R. Gow.** 1999. Regulatory networks controlling *Candida albicans* morphogenesis. Trends Microbiol. **7:**333–338.
5. **Calderone, R. A. (ed.).** 2002. *Candida* and candidiasis. American Society for Microbiology, Washington, D.C.
6. **Dirick, L., T. Böhm, and K. Nasmyth.** 1995. Roles and regulation of Cln-Cdc28 kinases at the start of the cell cycle of *Saccharomyces cerevisiae*. EMBO J. **14:**4803–4813.
7. **Edgington, N. P., M. J. Blacketer, T. A. Bierwagen, and A. M. Myers.** 1999. Control of *Saccharomyces cerevisiae* filamentous growth by cyclin-dependent kinase Cdc28. Mol. Cell. Biol. **19:**1369–1380.
8. **Edmond, M. B., S. E. Wallace, D. K. McClish, M. A. Pfaller, R. N. Jones, and R. P. Wenzel.** 1999. Nosocomial bloodstream infections in United States hospitals: a three-year analysis. Clin. Infect. Dis. **29:**239–244.
9. **Futcher, B.** 1996. Cyclins and the wiring of the yeast cell cycle. Yeast **12:** 1635–1646.
10. **Gilfillan, G. D., D. J. Sullivan, K. Haynes, T. Parkinson, D. C. Coleman, and N. A. R. Gow.** 1998. *Candida dubliniensis*: phylogeny and putative virulence factors. Microbiology **144:**829–838.
11. **Gimeno, C. J., P. O. Ljungdahl, C. A. Styles, and G. R. Fink.** 1992. Unipolar cell divisions in the yeast *S. cerevisiae* lead to filamentous growth: regulation by starvation and RAS. Cell **68:**1077–1090.
12. **Gomes de Mesuita, D., R. ten Hoopen, and C. L. Woldringh.** 1991. Vacuolar segregation to the bud of *Saccharomyces cerevisiae*: an analysis of morphology and timing in the cell cycle. J. Gen. Microbiol. **137:**2447–2454.
13. **Gow, N. A. R.** 1997. Germ tube growth of *Candida albicans*. Curr. Top. Med. Mycol. **8:**43–55.
14. **Gow, N. A. R.** 2002. Cell biology and cell cycle of *Candida albicans*, p. 145–158. *In* R. A. Calderone (ed.), *Candida* and candidiasis. American Society for Microbiology, Washington, D.C.
15. **Gow, N. A. R., and G. W. Gooday.** 1982. Growth kinetics and morphology of colonies of the filamentous form of *Candida albicans*. J. Gen. Microbiol. **128:**2187–2194.
16. **Gow, N. A. R., and G. W. Gooday.** 1982. Vacuolation, branch production and linear growth of germ tubes in *Candida albicans*. J. Gen. Microbiol. **128:** 2195–2198.
17. **Gow, N. A. R., and G. W. Gooday.** 1987. Cytological aspects of dimorphism in *Candida albicans*. Crit. Rev. Microbiol. **15:**73–78.
18. **Gow, N. A. R., G. W. Gooday, R. Newsam, and K. Gull.** 1980. Ultrastructure of the septum of *Candida albicans*. Curr. Microbiol. **4:**357–359.
19. **Gow, N. A. R., G. Henderson, and G. W. Gooday.** 1986. Cytological interrelationships between the cell cycle and duplication cycle of *Candida albicans*. Microbios **47:**97–105.
20. **Gow, N. A. R., A. J. P. Brown, and F. C. Odds.** 2002. Fungal morphogenesis and host invasion. Curr. Opin. Microbiol. **5:**366–371.
21. **Gray, D. I., and B. M. Morris.** 1992. A low cost video analysis system for the BBC master computer. Binary **4:**58–61.
22. **Hamer, J. E., J. A. Morrell, L. Hamer, T. Wolkow, and M. Momany.** 1999. Cellularization in *Aspergillus nidulans*, p. 201–228. *In* N. A. R. Gow, G. D. Robson, and G. M. Gadd (ed.). The fungal colony. Cambridge University Press, Cambridge, United Kingdom.
23. **Hazan, I., M. Sepulveda-Becerra, and H. Liu.** 2002. Hyphal elongation is regulated independently of cell cycle in *Candida albicans*. Mol. Biol. Cell **13:**134–145.

24. **Hedden, D. M., and J. D. Buck.** 1980. A re-emphasis—germ tubes diagnostic for *Candida albicans* have no constrictions. Mycopathologia **70:**95–101.
25. **Heid, P., E. Voss, and D. R. Soll.** 2003. 3D-DIASemb: a computer-assisted system for reconstructing and motion analyzing in 4D every cell and nucleus in a developing embryo. Dev. Biol. **245:**329–347.
26. **Hill, K. L., N. L. Catlett, and L. S. Weisman.** 1996. Actin and myosin function in directed vacuole movement during yeast cell division in *Saccharomyces cerevisiae*. J. Cell Biol. **135:**1535–1549.
27. **Hoch, H. C., R. C. Staples, B. Whitehead, J. Comeau, and E. D. Wolf.** 1987. Signalling for growth orientation and cell differentiation by surface topography in *Uromyces*. Science **235:**1659–1662.
28. **Holmes, A. R., R. D. Cannon, and M. G. Shepherd.** 1992. Mechanisms of aggregation accompanying morphogenesis in *Candida albicans*. Oral Microbiol. Immunol. **7:**32–37.
29. **Hube, B., and J. Naglik.** 2001. *Candida albicans* proteinases: resolving the mystery of a gene family. Microbiology **147:**1997–2005.
30. **Hube, B., M. Monod, D. A. Schofield, A. J. P. Brown, and N. A. R. Gow.** 1994. Expression of seven members of the gene family encoding secretory aspartyl proteinases in *Candida albicans*. Mol. Microbiol. **14:**87–99.
31. **Jorgensen, P., J. L. Nishikawa, B. J. Breitkreutz, and M. Tyers.** 2002. Systematic identification of pathways that couple cell growth and division in yeast. Science **297:**395–400.
32. **Kron, S. J.** 2002. Time-lapse microscopy of yeast cell growth. Methods Enzymol. **351:**3–15.
33. **Kron, S. J., C. A. Styles, and G. R. Fink.** 1994. Symmetric cell division in pseudohyphae of the yeast *Saccharomyces cerevisiae*. Mol. Biol. Cell **5:**1003–1022.
34. **Kron, S. J., and N. A. R. Gow.** 1995. Budding yeast morphogenesis: signalling, cytoskeleton and cell cycle. Curr. Opin. Cell Biol. **7:**845–855.
35. **Kwon, Y. H., H. C. Hoch, and J. R. Aist.** 1991. Initiation of appressorium formation in *Uromyces appendiculatus*: organization of the apex, and the responses involving microtubules and apical vesicles. Can. J. Bot. **69:**2560–2573.
36. **Lee, K. L., H. R. Buckley, and C. C. Campbell.** 1975. An amino acid liquid synthetic medium for the development of mycelial and yeast forms of *Candida albicans*. Sabouraudia **13:**148–153.
37. **Lew, D. J.** 2000. Cell cycle checkpoint that ensures coordination between nuclear and cytoplasmic events in *Saccharomyces cerevisiae*. Curr. Opin. Genet. Dev. **10:**47–53.
38. **Lew, D. J., and S. T. Reed.** 1993. Morphogenesis in the yeast cell cycle: regulation by Cdc28 and cyclins. J. Cell Biol. **120:**1305–1320.
39. **Lew, D. J., and S. T. Reed.** 1995. Cell cycle control of morphogenesis in budding yeast. Curr. Opin. Genet. Dev. **5:**17–23.
40. **Lo, H. J., J. R. Kohler, B. DiDomenico, D. Loebenberg, A. Cacciapuoti, and G. R. Fink.** 1997. Nonfilamentous C. albicans mutants are avirulent. Cell **90:**939–949.
41. **Loeb, J. D. J., M. Sepulveda-Becerra, I Hazan, and H. Liu.** 1999. A G_1 cyclin is necessary for maintenance of filamentous growth in *Candida albicans*. Mol. Cell. Biol. **19:**4019–4027.
42. **Martin, M. V., G. T. Craig, and D. J. Lamb.** 1984. An investigation of the role of true hypha production in the pathogenesis of experimental oral candidosis. Sabouraudia **22:**471–476.
43. **McCarthy, P. J., L. J. Nisbet, J. C. Boehm, and W. D. Kingsbury.** 1985. Multiplicity of peptide permeases in *Candida albicans*: evidence from novel chromophoric peptides. J. Bacteriol. **162:**1024–1029.
44. **McMillan, J. N., M. S. Longtine, R. A. Sia, C. L. Theesfeld, E. S. Bardes, J. R. Pringle, and D. J. Lew.** 1998. A morphogenesis checkpoint monitors the actin cytoskeleton in yeast. J. Cell Biol. **142:**1487–1499.
45. **Mendenhall, M. D., and A. E. Hodge.** 1998. The regulation of Cdc28 cyclin-dependent protein kinase activity during the cell cycle of the yeast *Saccharomyces cerevisiae*. Microbiol. Mol. Biol. Rev. **62:**1191–1243.
46. **Mitchison, J. M., and P. Nurse.** 1985. Growth in cell length in the fission yeast *Schizosaccharomyces pombe*. J. Cell Sci. **75:**357–376.
47. **Odds, F. C.** 1988. Candida and candidosis. Ballière Tindall, London, United Kingdom.
48. **Odds, F. C., L. Van Nuffel, and N. A. R. Gow.** 2000. Survival in experimental *Candida albicans* infections depends on inoculum growth conditions as well as animal hosts. Microbiology **146:**1881–1889.
49. **Odds, F. C., N. A. R. Gow, and A. P. J. Brown.** 2001. Fungal virulence studies come of age. Genome Biol. **2:**1009.1–1009.4.
50. **Prosser, J. I., and A. J. Taylor.** 1991. Growth mechanisms and growth kinetics of filamentous microorganisms. Crit. Rev. Biotechnol. **10:**253–274.
51. **Ritz, K., and J. W. Crawford.** 1999. Colony development in nutritionally heterogeneous environments, p. 49–74. *In* N. A. R. Gow, G. D. Robson, and G. M. Gadd (ed.), The fungal colony. Cambridge University Press, Cambridge, United Kingdom.
52. **Robinow, C. F.** 1963. Observations on cell growth, mitosis, and division in the fungus *Basidiobolus ranarum*. J. Cell Biol. **17:**123–152.
53. **Rupeš, I.** 2002. Checking cell size in yeast. Trends Genet. **18:**479–485.
54. **Ryley, J. F., and N. G. Ryley.** 1990. *Candida albicans*—do mycelia matter? J. Med. Vet. Mycol. **28:**225–239.
55. **Sevilla, M-J., and F. C. Odds.** 1986. Development of *Candida albicans* hyphae in different growth media—variations in growth rates, cell dimensions and timing of morphogenetic events. J. Gen. Microbiol. **132:**3083–3088.
56. **Sherman, F.** 1991. Getting started with yeast. Methods Enzymol. **194:**3–21.
57. **Sheu, Y.-J., and M. Snyder.** 2001. Control of cell polarity and shape, p 19–53. *In* R. J. Howard and N. A. R. Gow (ed.), The mycota VIII. Springer-Verlag, Heidelberg, Germany.
58. **Sobel, J. D., G. Muller, and H. R. Buckley.** 1984. Critical role of germ tube formation in the pathogenesis of candidal vaginitis. Infect. Immun. **44:**576–580.
59. **Soll, D. R., and L. H. Mitchell.** 1983. Filament ring formation in the dimorphic yeast *Candida albicans*. J. Cell Biol. **96:**486–493.
60. **Soll, D. R., M. Stasi, and G. Bedell.** 1978. The regulation of nuclear migration and division during pseudo-mycelium outgrowth in the dimorphic yeast *Candida albicans*. Expr. Cell Res. **116:**201–215.
61. **Soll, D. R., and E. Voss.** 1998. Two and three dimensional computer systems for analyzing how cells crawl, p. 25–52. *In* D. R. Soll and D. Wessels (ed.), Motion analysis of living cells. John Wiley, Inc., New York, N.Y.
62. **Soll, D. R., E. Voss, O. Johnson, and D. J. Wessels.** 2000. Computer assisted systems for the 4D reconstruction and analysis of living cells, nuclei, pseudopods, vesicle and molecular complexes. Scanning **22:**249–257.
63. **Staebell, M., and D. R. Soll.** 1985. Temporal and spatial differences in cell wall expansion during bud and mycelium formation in *Candida albicans*. J. Gen. Microbiol. **131:**1467–1480.
64. **Steinberg, G., M. Schliwa, C. Lehmler, M. Bölker, R. Kahmann, and J. R. McIntosh.** 1998. Kinesin from the plant pathogenic fungus *Ustilago maydis* is involved in vacuole formation and cytoplasmic migration. J. Cell Sci. **111:**2235–2246.
65. **Sudbery, P. E.** 2001. The germ tubes of *Candida albicans* hyphae and pseudohyphae show different patterns of septin ring localization. Mol. Microbiol. **41:**19–31.
66. **Sylwester, A., K. Daniels, and D. R. Soll.** 1998. The invasive and destructive behavior of HIV-induced T cell syncytia on collagen and endothelium. J. Leukoc. Biol. **32:**233–244.
67. **Takeo, K., R. Tanaka, H. Taguchi, and K. Nishimura.** 1993. Analysis of ploidy and sexual characteristics of natural isolates of *Cryptococcus neoformans*. Can. J. Microbiol. **39:**958–963.
68. **Trinci, A. P. J., M. G. Weibe, and R. D. Robson.** 1994. The mycelium as an integrated entity, p. 175–193. *In* J. G. H. Wessels and H. Meinhardt (ed.), The mycota I. Springer-Verlag, Heidelberg, Germany.
69. **Turner, G., and S. D. Harris.** Genetic control of polarized growth and branching in filamentous fungi, p. 229–260. *In* N. A. R. Gow, G. D. Robson, and G. M. Gadd (ed.), The fungal colony. Cambridge University Press, Cambridge, United Kingdom.
70. **Tyers, M., G. Tokiwa, and B. Futcher.** 1993. Comparison of the *Saccharomyces cerevisiae* G1 cyclins: Cln3 may be an upstream activator of Cln1, Cln2 and other cyclins. EMBO J **12:**1955–1968.
71. **Vida, T. A., and S. D. Emr.** 1995. A new vital stain for visualizing vacuolar membrane dynamics and endocytosis in yeast. J. Cell Biol. **128:**779–792.
72. **Weisman, L. S., R. Bacallao, and W. Wickner.** 1987. Multiple methods of visualizing the yeast vacuole permit evaluation of its morphology and inheritance during the cell cycle. J. Cell Biol. **105:**1539–1547.
73. **Wessels, D., E. Voss, N. Von Bergen, R. Burns, J. Stites, and D. R. Soll.** 1998. A computer-assisted system for reconstructing and interpreting the dynamic three dimensional relationships of the outer surface, nucleus and pseudopods of crawling cells. Cell Motil. Ctytoskel. **41:**225–246.
74. **Wolkow, T. D., S. D. Harris, and J. E. Hamer.** 1996. Cytokinesis in *Aspergillus nidulans* is controlled by cell size, nuclear positioning and mitosis. J. Cell Sci. **109:**2179–2188.
75. **Yokoyama, K., and K. Takeo.** 1983. Differences of asymmetrical division between the pseudomycelial and yeast forms of *Candida albicans* and their effect on multiplication. Arch. Microbiol. **134:**251–253.
76. **Zhang, Z., Z. He, and G. Guan.** 1999. Thermal stability and thermodynamic analysis of native and methoxypolyethylene glycol modified trypsin. Biotechnol. Technol. **13:**781–786.